

DREAM: a fluid-kinetic framework for tokamak disruption runaway electron simulations

M. Hoppe, O. Embreus and T. Fülöp

Department of Physics, Chalmers University of Technology, Göteborg, Sweden

Relativistic runaway electrons (RE) created by strong electric fields induced during the current quench (CQ) phase of a tokamak disruption pose a significant threat to future reactor-scale devices. Since the number of runaway electrons generated is exponentially sensitive to the plasma current of the tokamak [1], the robustness of any proposed RE prevention or mitigation scheme cannot be verified experimentally on today's medium-size tokamaks, requiring that comprehensive, self-consistent and validated models be utilized for predictions. In this contribution we present the new code DREAM (for *Disruption Runaway Electron Analysis Model*) [2] which is designed specifically for studying the generation of runaway electrons during tokamak disruptions. The tool couples a set of 1D fluid plasma models with a 1D2P bounce-averaged Fokker–Planck model for the electron population, allowing both runaway electrons and parameters essential to their generation to be evolved self-consistently.

Electron treatment During tokamak disruptions, electrons will typically evolve on three separate energy scales. Most electrons successfully cool down in the thermal quench (TQ), forming a *cold* Maxwellian population at a temperature $T_{\text{cold}} \sim 1 \text{ eV}$ after the TQ. The most energetic electrons in the initially warm plasma may however not be able to cool down sufficiently fast during the TQ, leaving them close to the critical momentum for runaway acceleration $p_c \sim mc\sqrt{E_c/E_{\parallel}} \sim 10 \text{ keV}/c$ when the CQ sets in and induces a strong electric field [3]. Once accelerated, these electrons enter the third energy regime, namely that of relativistic runaway electrons with momenta up to $p \sim 100 \text{ MeV}/c$. DREAM allows electrons in each of these three energy regimes to be evolved separately as fluids or using a kinetic equation. The kinetic equation used in DREAM is bounce-averaged and accounts for various processes important to runaway electron dynamics, including partial screening of ions [4], bremsstrahlung and synchrotron radiation losses, large-angle collisions, and radial transport.

Background plasma A set of 1D fluid models are used in DREAM for evolving background plasma quantities: electric field, poloidal flux, current density, ion density, ion temperature and

electron temperature. The first three are closely connected via Ampère's law

$$2\pi\mu_0 \langle \mathbf{B} \cdot \nabla \phi \rangle \frac{j_{\text{tot}}}{B} = \frac{1}{V'} \frac{\partial}{\partial r} \left[V' \left\langle \frac{|\nabla r|^2}{R^2} \right\rangle \frac{\partial \psi}{\partial r} \right], \quad (1)$$

where μ_0 is the vacuum permittivity, \mathbf{B} the magnetic field with strength $B = |\mathbf{B}|$, ϕ the toroidal angle, j_{tot} the total current density, ψ the poloidal flux, R the major radius coordinate and r a flux surface label. Angle brackets denote a flux-surface average $\langle X \rangle = (1/V') \int_0^{2\pi} d\phi \int_{-\pi}^{\pi} d\theta \mathcal{J} X$, with \mathcal{J} the configuration space Jacobian, and $V' = \int_0^{2\pi} d\phi \int_{-\pi}^{\pi} d\theta \mathcal{J}$. The electric field $\langle \mathbf{E} \cdot \mathbf{B} \rangle / \langle \mathbf{B} \cdot \nabla \phi \rangle = V_{\text{loop}}/2\pi$ is coupled to equation (1) via

$$\frac{\partial \psi}{\partial t} = -V_{\text{loop}} + \frac{\partial}{\partial \psi_t} \left(\psi_t \mu_0 \Lambda \frac{\partial}{\partial \psi_t} \frac{j_{\text{tot}}}{B} \right) \quad (2)$$

The second term in equation (2) represents hyperresistive diffusion [5] and acts to flatten the current profile due to magnetic field line breaking.

The total current density $j_{\text{tot}} = j_{\Omega} + j_{\text{hot}} + j_{\text{re}}$ contains separate contributions from all three electron energy regions simulated. The RE current density $j_{\text{re}} = ecn_{\text{re}}$, where e is the elementary charge and c is the speed of light, while the hot electron current density is calculated as the current moment of the hot electron distribution function

$$\frac{j_{\text{hot}}}{B} = -\frac{2\pi e}{B_{\min}} \int_{p_{\text{hot}}}^{p_{\text{re}}} dp \int_{-1}^1 d\xi_0 p^2 \mathcal{H}(\xi_0) v \xi_0 f_{\text{hot}}(r, p, \xi_0). \quad (3)$$

Here, $\mathcal{H}(\xi_0)$ is zero in the trapping region and one outside. The current carried by the Maxwellian-distributed cold electrons is obtained from a modified Ohm's law

$$\frac{j_{\Omega}}{B} = \sigma \frac{\langle \mathbf{E} \cdot \mathbf{B} \rangle}{\langle B^2 \rangle} + \frac{\delta j_{\text{corr}}}{B}, \quad (4)$$

where the correction term δj_{corr} is necessary to account for transient currents when the cold electrons are modelled kinetically, since DREAM uses a test-particle collision operator.

The thermal energy $W_{\text{cold}} = 3\langle n_{\text{cold}} \rangle T_{\text{cold}}/2$ of the cold electron population is evolved using

$$\begin{aligned} \frac{\partial W_{\text{cold}}}{\partial t} &= \frac{j_{\Omega}}{B} \langle \mathbf{E} \cdot \mathbf{B} \rangle - \langle n_{\text{cold}} \rangle \sum_i \sum_{j=0}^{Z_i-1} n_i^{(j)} L_i^{(j)} + \langle Q_c \rangle \\ &\quad + \frac{1}{V'} \frac{\partial}{\partial r} \left[V' \frac{3\langle n_{\text{cold}} \rangle}{2} \left(A_W T_{\text{cold}} + D_W \frac{\partial T_{\text{cold}}}{\partial r} \right) \right] \end{aligned} \quad (5)$$

where the terms represent ohmic heating, inelastic losses, collisional heat transfer and radial transport, respectively. The rate of energy loss by inelastic atomic processes $L_i^{(j)}$ includes line and recombination radiation, bremsstrahlung, as well as accounting for the change in potential energy due to excitation and recombination. The collisional energy transfer term accounts for energy transfer between electrons and ions, as well as between the various electron populations.

DREAM simulations can include an arbitrary number of ion species, and the charge states j of each species i are evolved according to

$$\frac{\partial n_i^{(j)}}{\partial t} = \left(I_i^{(j-1)} \langle n_{\text{cold}} \rangle + \left\langle \sigma_{\text{ion},i}^{(j-1)} v \right\rangle \right) n_i^{(j-1)} + \left(I_i^{(j)} \langle n_{\text{cold}} \rangle + \langle \sigma_{\text{ion},i} v \rangle \right) n_i^{(j)} + R_i^{(j+1)} \langle n_{\text{cold}} \rangle n_i^{(j+1)} - R_i^{(j)} \langle n_{\text{cold}} \rangle n_i^{(j)}, \quad (6)$$

with ionization and recombination coefficients $I_i^{(j)}$ and $R_i^{(j)}$ taken from the OpenADAS database [6]. The kinetic ionization rates are calculated as moments of the electron distribution function, allowing DREAM to account for fast electron impact ionization with self-consistently evolved fast electron distribution functions.

Hot-tail generation An important feature of DREAM is its broad capabilities for modelling RE generation via the so-called hot-tail mechanism [3]. In particular, the flexible treatment of the various electron sub-populations (as described above) leads to four primary models for hot-tail generation, here referred to as *fluid*, *fully kinetic*, *superthermal* and *isotropic*.

The *fluid* model has a fluid cold electron population, a fluid RE population and no separate hot population. In a disruption simulation, as cold gas enters the plasma, the initially warm electrons cool down to the post-TQ temperature. Runaways generated via the hot-tail mechanism are added to the RE density n_{RE} using a fluid source term [7]. In contrast, the *fully kinetic* model resolves the full radius-energy-pitch distribution function $f(r, p, \xi_0)$ of both the cold, hot and runaway electrons. This means that any generation of RE via the hot-tail mechanism results from the collisional processes described by the kinetic equation. For the kinetic equation, a test-particle operator evaluated at a separately evolved cold electron temperature T_{cold} , as in equation (5), is used. The temperature T_{cold} starts at the pre-disruption temperature and is then dynamically evolved towards the final post-disruption temperature.

The *superthermal* model, first considered in Ref. [8], assumes that cold impurities entering the plasma at the onset of the disruption will release zero-temperature electrons that immediately form a cold Maxwellian population. The cold electrons are therefore only represented by a dynamically evolving cold electron density and temperature. Hot electrons are however represented by a hot electron distribution, evolved using a kinetic equation expanded in the superthermal ($p \gg p_{\text{th}}$) limit, and colliding only with cold electrons. Before the disruption, all electrons are situated in the hot population. Runaway generation through the hot-tail mechanism is therefore treated kinetically also in the *superthermal* model, but with the added assumption of the electrons exhibiting a two-component behaviour during the TQ, which could otherwise cause the *fully kinetic* model to break down. The related *isotropic* model is an extension of

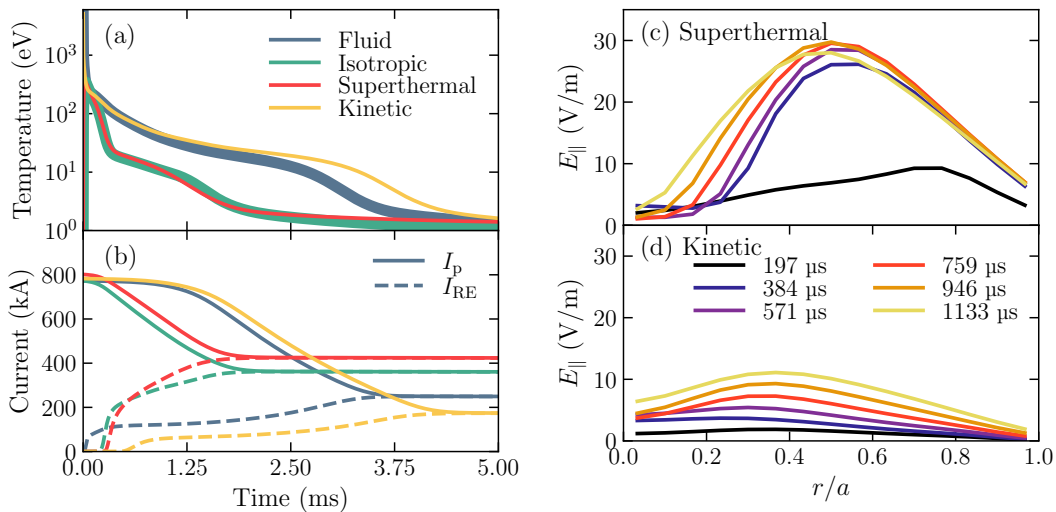


Figure 1: Comparison of the four electron models considered here. Some differences between the *fluid/kinetic* and *superthermal/isotropic* models can be seen, mainly due to the differing treatment of the electron temperature, resulting in (b) different electric field evolutions.

the *superthermal* model where the kinetic equation has also been integrated over pitch angle. Hence, the *isotropic* model only considers the energy distribution of the hot electrons.

Comparison of electron models Figures 1a and b show the plasma current evolution with the four hot-tail models described above in an ASDEX Upgrade-like plasma with $T_{e,0} = 5.8$ keV, $n_{e,0} = 2.6 \times 10^{19} \text{ m}^{-3}$ and $I_{p,0} = 800$ kA [2]. In the simulation, a combination of $n_D = 5.2 \times 10^{20} \text{ m}^{-3}$ deuterium and $n_{\text{Ar}} = 5.2 \times 10^{18} \text{ m}^{-3}$ argon is inserted radially uniformly in the plasma at $t = 0$. The resulting plasma evolution reveals reasonable agreement between the *fluid* and *kinetic* models, as well as between the *superthermal* and *isotropic* models, but not between the two groups of models. The differences in results between the two groups of models stems from the different temperatures used for the collisional electron background, which starts at the pre-disruption temperature in the two former, and at zero temperature in the two latter, resulting in different electric field evolutions as shown in figures 1c and d.

References

- [1] Rosenbluth M. and Putvinski. S, Nucl. Fusion **37** 1355 (1997)
- [2] Hoppe M., Embreus O. and Fülöp T., submitted to Comp. Phys. Comm. (2021) arXiv:2103.6457
- [3] Smith H. and Verwichte E., Phys. Plasmas **15** 072502 (2008)
- [4] Hesslow L. *et al*, J. of Plasma Phys. **84** 905840605 (2018)
- [5] Boozer A. H., J. Plasma Phys. **35** 133-139 (1986)
- [6] Summers H. P., The ADAS User Manual version 2.6 (2004) <http://www.adas.ac.uk>
- [7] Svenningsson I., MSc Thesis, Chalmers University of Technology (2020)
- [8] Aleynikov P. and Breizman B., Nucl. Fusion **57** 046009 (2017)
- [9] Svenningsson I. *et al*, accepted in Phys. Rev. Lett. (2021) arXiv:2104.03272